UC Berkeley
UC Berkeley Previously Published Works

Title

Toxic heavy metal – Pb, Cd, Sn – complexation by the octadentate hydroxypyridinonate ligand archetype 3,4,3-LI(1,2-HOPO)

Permalink

https://escholarship.org/uc/item/7rj2v1p9

Journal

New Journal of Chemistry, 42(10)

ISSN

1144-0546

Authors

Deblonde, Gauthier J-P
Lohrey, Trevor D
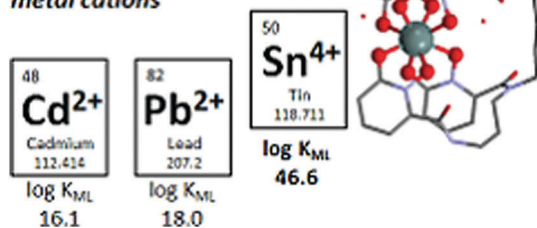An, Dahlia D
et al.

Publication Date

2018

DOI

10.1039/c7nj04559j

Peer reviewed

We have presented the Graphical Abstract text and image for your article below. This brief summary of your work will appear in the contents pages of the issue in which your article appears.

Toxic heavy metal – Pb, Cd, Sn – complexation by the octadentate hydroxypyridinonate ligand archetype 3,4,3-LI(1,2-HOPO)   Q1

Gauthier J.-P. Deblonde, Trevor D. Lohrey, Dahlia D. An and Rebecca J. Abergel   Q3

The toxicity of heavy metals such as lead (Pb), cadmium (Cd) and tin (Sn) has long been known but accidental exposures of large populations to these elements remain unfortunately a topical issue.   Q5

Please check this proof carefully. **Our staff will not read it in detail after you have returned it.**

Proof corrections must be returned as a single set of corrections, approved by all co-authors. No further corrections can be made after you have submitted your proof corrections as we will publish your article online as soon as possible after they are received.

Please ensure that:
- The spelling and format of all author names and affiliations are checked carefully. Names will be indexed and cited as shown on the proof, so these must be correct.
- Any funding bodies have been acknowledged appropriately.
- All of the editor's queries are answered.
- Any necessary attachments, such as updated images or ESI files, are provided.

Translation errors between word-processor files and typesetting systems can occur so the whole proof needs to be read. Please pay particular attention to: tables; equations; numerical data; figures and graphics; and references.

Please send your corrections preferably as a copy of the proof PDF with electronic notes attached or alternatively as a list of corrections – do not change the text within the PDF file or send a revised manuscript. Corrections at this stage should be minor and not involve extensive changes.

Please return your **final** corrections, where possible within **48 hours** of receipt, by e-mail to: njc@rsc.org. If you require more time, please notify us by email.

Funder information

Providing accurate funding information will enable us to help you comply with your funders' reporting mandates. Clear acknowledgement of funder support is an important consideration in funding evaluation and can increase your chances of securing funding in the future. We work closely with Crossref to make your research discoverable through the Funding Data search tool (http://search.crossref.org/funding).

Further information on how to acknowledge your funders can be found on our webpage (http://rsc.li/funding-info).

What is Funding Data?

Funding Data (http://www.crossref.org/fundingdata/) provides a reliable way to track the impact of the work that funders support. We collect funding information from our authors and match this information to funders listed in the Crossref Funder Registry. Once an article has been matched to its funders, it is discoverable through Crossref's search interface.

PubMed Central

Accurate funder information will also help us identify articles that are mandated to be deposited in PubMed Central (PMC) and deposit these on your behalf.

Providing funder information

We have combined the information you gave us on submission with the information in your acknowledgements. This will help ensure funding information is as complete as possible and matches funders listed in the Crossref Funder Registry. **Please check that the funder names and grant numbers in the table are correct.** This table will not be included in your final PDF but we will share the data with Crossref so that your article can be found *via* the Funding Data search tool.

Funder name	Funder ID (for RSC use only)	Award/grant/contract number
Office of Science	100006132	DE-AC02-05CH11231

If a funding organisation you included in your acknowledgements or on submission of your article is not currently listed in the registry it will not appear in the table above. We can only deposit data if funders are already listed in the Crossref Funder Registry, but we will pass all funding information on to Crossref so that additional funders can be included in future.

Researcher information

If any authors have ORCID or ResearcherID details that are not listed below, please provide these with your proof corrections. Please check that the ORCID and ResearcherID details listed below have been assigned to the correct author. Authors should have their own unique ORCID iD and should not use another researcher's, as errors will delay publication.

Please also update your account on our online manuscript submission system to add your ORCID details, which will then be automatically included in all future submissions. See here for step-by-step instructions and more information on author identifiers.

First (given) name(s)	Last (family) name(s)	ResearcherID	ORCID
Gauthier J.-P.	Deblonde	O-3881-2014	0000-0002-0825-8714
Trevor D.	Lohrey		0000-0003-3568-7861
Dahlia D.	An		0000-0002-8763-6735
Rebecca J.	Abergel		0000-0002-3906-8761

Queries for the attention of the authors

Journal: **NJC**

Paper: **c7nj04559j**

Title: **Toxic heavy metal – Pb, Cd, Sn – complexation by the octadentate hydroxypyridinonate ligand archetype 3,4,3-LI(1,2-HOPO)**

For your information: You can cite this article before you receive notification of the page numbers by using the following format: (authors), New J. Chem., (year), DOI: 10.1039/c7nj04559j.

Editor's queries are marked on your proof like this **Q1**, **Q2**, etc. and for your convenience line numbers are indicated like this 5, 10, 15, …

Please ensure that all queries are answered when returning your proof corrections so that publication of your article is not delayed.

Query reference	Query	Remarks
Q1	Please confirm that the spelling and format of all author names is correct. Names will be indexed and cited as shown on the proof, so these must be correct. No late corrections can be made.	
Q2	Please check that the inserted CCDC number is correct.	
Q3	Do you wish to indicate the corresponding author(s)? If so, please specify the corresponding author(s).	
Q4	Do you wish to add an e-mail address for the corresponding author? If so, please provide the relevant information.	
Q5	Please check that the inserted Graphical Abstract text is suitable. Please ensure that the text fits between the two horizontal lines.	
Q6	Please note that a conflict of interest statement is required for all manuscripts. Please read our policy on Conflicts of interest (http://rsc.li/conflicts) and provide a statement with your proof corrections. If no conflicts exist, please state that "There are no conflicts to declare".	
Q7	Ref. 14 and 33: Can these references be updated? If so, please provide the relevant information such as year, volume and page or article numbers as appropriate.	
Q8	Ref. 39: Please provide the patent type and patent number.	

Toxic heavy metal – Pb, Cd, Sn – complexation by the octadentate hydroxypyridinonate ligand archetype 3,4,3-LI(1,2-HOPO)†

Gauthier J.-P. Deblonde, [a] Trevor D. Lohrey, [ab] Dahlia D. An [a] and Rebecca J. Abergel [ac]

The toxicity of heavy metals such as lead (Pb), cadmium (Cd) and tin (Sn) has long been known but accidental exposures of large populations to these elements remain unfortunately a topical issue. Chelating agents against Pb, Cd, or Sn poisoning are still limited to classical ligands such as ethylenediamine tetraacetic acid (EDTA). Here, we evaluate the ability of 3,4,3-LI(1,2-HOPO) (L^{4-}), an octadentate ligand currently under evaluation for actinide decorporation, to bind Pb, Cd and Sn metal ions in aqueous solutions. This ligand forms 1:1 complexes with Pb(II), Cd(II) and Sn(IV) as well as bimetallic 2:1 species with Pb(II) and Cd(II), all of which were characterized by high resolution mass spectrometry and spectrophotometric titrations. The 3,4,3-LI(1,2-HOPO) ligand exhibits an extreme affinity for Sn(IV) ions ($\log \beta_{110} > 40$), with the complex remaining stable from highly acidic conditions to alkaline media (from 3 M HCl to pH 8). Single crystals of the neutral complex [Sn^{IV}3,4,3-LI(1,2-HOPO)·$3H_2O$] were obtained and its structure determined, revealing a chiral conformation. Although not initially designed for hexacoordinated metals such as Pb(II) and Cd(II), the octadentate ligand shows promise for the *in vitro* or *in vivo* sequestration of toxic heavy metals, as evidenced by decorporation experiments performed in mice contaminated with ^{210}Pb(II) and treated with either EDTA or 3,4,3-LI(1,2-HOPO).

Introduction

Heavy metals such as lead (Pb), cadmium (Cd) and, to a lesser extent, tin (Sn) have long been suspected to have deleterious health effects on humans.[1,2] Pb-, Cd- and Sn-based chemicals are nonetheless essential to many contemporary applications such as battery components, pigments, alloys, control rods for nuclear reactors, or food cans. The historical use of Pb-based piping still represents a health hazard for some tap water systems and can lead, under particular circumstances, to the exposure of a large number of people to contaminated water, as unfortunately exemplified by the recent events in the North American State of Michigan.[3–5] Detectable levels of Pb have also been found in baby food.[6] The US Environmental Protection Agency set the "action level" on water systems to 15 ppb of Pb ($\sim$15 μg L^{-1} or 72 nM) in drinking water and the US Food and Drug Administration allows a maximum of 5 ppb of Pb in bottled water.[7] For Cd, the most significant sources of exposure for humans are considered to be the inhalation of cigarette smoke and industrial dusts.[8] Sn alloys are widely used to make cans and containers for long term storage of foods and beverages. Leaching of Sn alloys, especially if the material is not lacquered and if the beverage is acidic, slowly increases the level of Sn in the food stored inside the can. A study performed by the UK Ministry of Agriculture, Fisheries and Food found as much as 50–210 ppm of Sn (50–210 mg L^{-1} or 0.4–1.7 μM) in canned pineapple products sold in the UK.[9] Although less harmful than Pb and Cd, the toxicity of Sn is still subject to debate and seems to be highly compound dependent. Clinical studies have shown that the consumption of food containing a high level of Sn causes acute nausea and gastrointestinal disorders.[9] Post-treatment of heavy metal poisoning is usually addressed by chelation therapy and, most of the time, ethylenediaminetetraacetate salts (EDTA) are used. In some cases, such as for Cd, EDTA is contraindicated as it increases metal-induced renal damage due to the excretion of the complex through the urinary pathway.[2] Hence, the quest for better chelators amenable to chelate and safely excrete hazardous elements from the body is still a subject of interest.

We here present an evaluation of the octadentate ligand, 3,4,3-LI(1,2-HOPO) for its affinity towards Pb^{2+}, Cd^{2+} and Sn^{4+}

[a] *Chemical Sciences Division, Lawrence Berkeley National Laboratory, Berkeley, CA 94720, USA*

[b] *Department of Chemistry, University of California, Berkeley, CA 94720, USA*

[c] *Department of Nuclear Engineering, University of California, Berkeley, CA 94720, USA*

ions in aqueous media. The design of 3,4,3-LI(1,2-HOPO) was inspired by natural iron(III)-seeking molecules and consists of a spermine backbone and four 1-hydroxypyridin-2-one (1,2-HOPO) binding units that are deprotonated at physiological pH.[10] It was recently demonstrated that this water-soluble ligand exhibits high affinity and selectivity for the sequestration, both *in vitro* and *in vivo*, of tetravalent f-elements (Ce^{4+}, Th^{4+}, Pu^{4+}, Bk^{4+}), trivalent lanthanides, and bivalent uranyl cations.[11–14] Its low toxicity and oral availability, as opposed to polyaminocarboxylate chelating agents such as EDTA and diethylenetriamine pentaacetic acid (DTPA), also make 3,4,3-LI(1,2-HOPO) an ideal therapeutic compound for future treatments against contamination with 4f or 5f elements, as reinforced by its current status as an Investigational New Drug in the US Recent studies have also shown that 3,4,3-LI(1,2-HOPO) is amenable to bind Zr^{4+} with extremely high affinity,[13] which led to the development of a promising bifunctional derivative for radiopharmaceutical applications, including [89]Zr-based positron emission tomography.[15,16] To the best of our knowledge, hydroxypyridinone-based ligands have not yet been considered for the chelation of Pb^{2+}, Cd^{2+} or Sn^{4+} ions. Herein, we assess the interactions of 3,4,3-LI(1,2-HOPO) with Pb, Cd, and Sn through aqueous solution thermodynamics, mass spectrometry, crystallography, and *in vivo* [210]Pb decorporation. This exploratory study lays the groundwork for the development of new bio-inspired chelating treatments of heavy metal poisoning.

Materials and methods

General considerations

All solutions were prepared using deionized water purified by a Millipore Milli-Q reverse osmosis cartridge system. $Pb(CH_3COO)_2 \cdot 3H_2O$ (99.995%, Alpha Aesar Puratronic), $CdCl_2$ (99.996% ultra-dry, Alpha Aesar), $SnCl_4 \cdot 5H_2O$ (99.7%, Acros Organics), and $ZrCl_4$ (99.5%, Beantown Chemicals) were used without further purification. Standard solutions of 0.1 M and 6.0 M HCl were purchased from BDH (VWR Analyticals). 3,4,3-LI(1,2-HOPO) was prepared as described previously.[17] All titrant solutions were degassed by boiling for 2 h while being purged under Ar. Carbonate-free 0.1 M KOH was prepared from concentrate (J. T. Baker Dilut-It) and was standardized by titrating against 0.1 M potassium hydrogen phthalate (99.95%, Sigma Aldrich). The glass electrode (Metrohm Micro Combi; response to $[H_3O^+]$) used for the pH measurements was calibrated at 25.0 °C and at an ionic strength of 0.1 M (KCl) before each spectrophotometric titration. The calibration data were analyzed using the program GLEE[18] to refine for the E° and slope. All thermodynamic measurements were conducted at 25.0 °C, in 0.1 M KCl supporting electrolyte under positive argon gas pressure (unless otherwise indicated). The automated titration system was controlled by an 867 pH Module (Metrohm). Two-milliliter Dosino 800 burets (Metrohm) dosed the titrant (0.1 M KOH or 0.1 M HCl) into the thermostated titration vessel containing 9 mL of sample. Static UV-visible spectra were measured using a Cary 5G spectrophotometer. UV-visible spectra for titrations were acquired with an Ocean Optics USB4000-UV-vis spectrophotometer equipped with a TP-300 dip probe (Ocean Optics; path length of 10 mm), fiber optics and a DH-2000 light source (deuterium and halogen lamps). The fully automated titration system and the UV-vis spectrophotometer were coordinated by LBNL titration system, a computer program developed in house for the coordination of the spectrophotometer, the titration burettes, and the pH-meter.

Mass spectrometry

High resolution mass spectra were acquired on a UPLC Waters Xevo system interfaced with a QTOF mass spectrometer (Waters Corporation, Milford, MA, USA) in Micromass Z-spray geometry. The mass spectrometer was equipped with an ESI source. Data acquisition and instrument control were accomplished using MassLynx software, version 4.1. Aqueous solutions containing 25 μM of the ligand and the metal of interest (metal/ligand = 1 mol mol^{-1}) were directly injected at a flow of 20 μL min^{-1} using a syringe pump (KD Scientific, Holliston, MA, USA). The voltage applied to the capillary was 3.00 and 2.50 kV in the positive and negative detection modes, respectively. A nitrogen gas flow rate of 30 L h^{-1} was used for the cone and 600 L h^{-1} for desolvatation. The cone voltage was set to 20 V in positive mode and 40 V in negative mode. The temperature was 80 °C for the ion source and 375 °C for desolvatation. Mass spectra were recorded over a 200–1200 m/z range over collection times of 1 min.

Incremental spectrophotometric titrations

This method was used to determine the formation constants of the 1:1 complexes formed between 3,4,3-LI(1,2-HOPO) and Pb(II) or Cd(II) as well as to assess the stability of the Sn(IV) complex between pH 2 and 12. Typically, 9 mL of a sample containing the ligand, 1.00 equivalent of the studied metal ion, and the supporting electrolyte were incrementally perturbed by addition of 0.020 mL of carbonate-free 0.1 M KOH followed by a time delay of 90 s. Buffering of the solution was ensured by the addition of 2 mM acetic acid, HEPES (4-(2-hydroxyethyl)-1-piperazineethanesulfonic acid), CHES (N-cyclohexyl-2-amino-ethanesulfonic acid) and MES (2-(N-morpholino)ethane-sulfonic acid). Between 120 and 240 data points were collected per titration, each data point consisting of a pH measurement and a UV-vis spectrum (240–450 nm) over the pH range ∼1.5 to ∼12. All spectra were corrected for dilution before data fitting. The entire procedure (electrode calibration, titration and data treatment) was performed independently at least three times for each metal–ligand complex.

Spectrophotometric batch titrations at constant pH

This method was used to determine the formation constants of the 1:2 complexes of 3,4,3-LI(1,2-HOPO) and Pb(II) or Cd(II) as well as the formation constant of the 1:1 complex [Sn^{IV}3,4,3-LI(1,2-HOPO)]. For the 2:1 Pb(II) and Cd(II) complexes, series of samples containing 20–30 μM of the ligand and an increasing amount of metal ions (from 1.00 to 35.0 equivalents) were

prepared in 10 mM formic acid buffer (I = 0.1 M, KCl). The pH values measured at equilibrium were comprised between 3.29 and 3.38. For the Sn(IV) complex, series of samples containing 30–40 μM of the ligand, 1.00 equivalent of $SnCl_4$ and from 0 to 1.00 equivalent of $ZrCl_4$ were prepared in 0.4 M HCl. Each series contained at least 10 samples which were equilibrated for 48 hours at 25.0 °C (Pb and Cd) or 20 °C (Sn) in a thermostated bath. UV-visible spectra were recorded after equilibrium and data were refined using HypSpec software.[19] At least three independent titrations were performed for each metal–ligand system.

Data treatment

Thermodynamic constants and spectral deconvolution were refined using the nonlinear least-squares fitting program Hyp-Spec. All equilibrium constants were defined as cumulative formation constants, β_{mlh} according to eqn (1) and (2), where the metal ion and deprotonated ligand are designated as M and L, respectively. All metal and ligand concentrations were held at estimated values determined from the volume of standardized stock solutions. All species formed with 3,4,3-LI(1,2-HOPO) were considered to have significant absorbance to be observed in the UV-vis spectra and were therefore included in the refinement process. The absorbance of $[SnCl_5]^-$ (major Sn species formed once the metal is unbound to 3,4,3-LI(1,2-HOPO) under the studied conditions) was also taken into account although it has almost no effect on the final $\log \beta_{110}$ value calculated for the HOPO complex due to the low extinction coefficient of this species. When publicly available, the stability constants of the chloride complexes (due to the chloride ions present in the buffer) were taken into account. The hydroxide and chloride complexes formation constants of the metal ions were taken from the NIST[20] or OECD[21,22] databases and systematically included in the refinement procedure. The refinements of the overall formation constants β_{mlh} also included previously determined ligand protonation constants.[10] Speciation diagrams or species distribution were calculated using the modeling program HYSS.[19] Uncertainties on $\log \beta_{mlh}$ and pK_a values presented in this paper correspond to the standard deviation observed over the n replicates (n = 3 to 4) of the entire procedure (electrode calibration, spectrophotometric measurement and data treatment).

$$mM + lL + hH \rightleftharpoons [M_mL_lH_h] \qquad (1)$$

$$\beta_{mlh} = \frac{[M_mL_lH_h]}{[M]^m[L]^l[H]^h} \qquad (2)$$

Crystallography

Single crystals of the Sn complex were obtained as follows. A methanol solution containing 2.8 μmol of 3,4,3-LI(1,2-HOPO) and 2.8 μmol $SnCl_4 \cdot 5H_2O$ was incubated at 55 °C for 2 h. After cooling to room temperature, the sample was slowly evaporated. Diamond shaped (Fig. S1, ESI†) single crystals of [Sn^{IV}3,4,3-LI(1,2-HOPO)·3H_2O] appeared after three weeks. Several of these crystals were transferred from their mother liquor,

suspended in paratone oil, and inspected under a microscope equipped with a polarizing filter. The crystals were cut into pieces of appropriate size, and a colorless shard of the dimensions 0.05 × 0.03 × 0.02 mm^3 was selected and mounted onto a 10 micron MiTiGen dual thickness MicroMount™. The mounted crystal was then immediately placed on the goniometer head of the diffractometer and cooled in a 100 K stream of dry nitrogen. Data collection was conducted at the Advanced Light Source station 11.3.1 at Lawrence Berkeley National Laboratory, using a silicon-monochromated beam of 16 keV (λ = 0.7749 Å) synchrotron radiation. The Bruker APEX3 software package (including SAINT and SADABS) was used throughout the data collection and reduction procedures.[23] The structure was determined and refined using SHELXT and SHELXL-2014 in the WinGX software package.[24,25] Figures of the finalized structure were generated using Mercury.[26] CCDC 1586746.†

In vivo evaluation

All procedures and protocols used in the presented *in vivo* studies were reviewed and approved by the Institutional Animal Care and Use Committee of the Lawrence Berkeley National Laboratory. Experiments were performed in compliance with guidelines from the Association for Assessment and Accreditation of Laboratory Animal Care International (AAALAC) and in AAALAC accredited facilities. The animals used were young adult [77 ± 1 (SD) days old, 29.3 ± 1.3 (SD) g] female Swiss-Webster mice (Simonsen Laboratories, Gilroy, CA, USA). Mice were kept under a 12 h light cycle with controlled temperature (18–22 °C) and relative humidity (30–70%), and were given water and food *ad libitum*. Each group of four mice was housed together in plastic stock cages lined with a 0.5 cm layer of highly absorbent low-ash pelleted cellulose bedding (Alpha-dry) for separation of urine and feces. Intravenous (iv) injections into a warmed lateral tail vein, intraperitoneal (ip) injections, and euthanasia were performed under isoflurane anesthesia. Ligand solutions were prepared such that the selected dosage (100 μmol kg^{-1}) was contained in 0.5 mL of 0.14 M NaCl, the pH being adjusted to 7.4–8.4 with 1 N NaOH. The metal challenge solution was prepared so that each 0.2 mL dose contained ^{210}Pb (925 Bq, 0.28 ng) in 0.008 M sodium citrate and 0.14 M NaCl, pH 4. To probe the effect of prophylactic treatment, groups of four mice were first administered ligand solutions ip at the following pre-contamination treatment times: 1 h, 6 h, 24 h. Mice were then injected a single iv dose of ^{210}Pb-citrate. To probe the effect of delayed treatment, groups of four mice were injected a single iv dose of ^{210}Pb-citrate, and ligand or isotonic saline solutions were administered ip at the following post-contamination treatment times: 1 h, 6 h, 24 h, 48 h. Excreta were collected daily until scheduled necropsy 4 days after the metal challenge. Mice were euthanized by cervical dislocation over their respective cage to collect the excreta expelled at death, and immediately wrapped in plastic and frozen for later dissection. All experiments were managed as metabolic balance studies, in which all tissues, and excreta were analyzed for ^{210}Pb by liquid scintillation counting

on a Perkin Elmer Packard Tri-Carb model B4430. The methods of sample collection, preparation, radioactivity measurements, and data reduction have been published previously.[27–30] The experimental data are reported as radionuclide fractions, expressed as percent of recovered ^{210}Pb (%RD), and values are arithmetic means $\pm$ SD. When comparing values between groups, the term "significant" is used in the statistical sense, indicating $p < 0.05$ by one-way analysis of variance (ANOVA) followed by a *post hoc* Dunnett's multiple-comparison test to compare groups of treated to the control group that was administered saline. All statistical analyses were performed using GraphPad Prism 5 (GraphPad Software, Inc., San Diego, CA, USA).

Results & discussion

Tin(IV) complex

In addition to its great ability to stabilize large tetravalent 4f and 5f cations such as Ce^{4+}, Th^{4+}, Pu^{4+}, and Bk^{4+},[11,13,14] the spermine-based hydroxypyridinone derivative offers a flexible backbone that, combined with its amine and amide groups, also accommodates smaller metals such as Zr^{4+}.[13,16] Sn^{4+} has no f-electrons and, with its ionic radius of 0.81 Å, is much smaller than the f-block ions mentioned above (ionic radii comprised between 1.05 and 0.93 Å) or Zr^{4+} (0.84 Å for a coordination number of 8).[31] Nonetheless, tetravalent Sn is amenable to form octacoordinated complexes which makes it a potential target for the four bidentate binding units of 3,4,3-LI(1,2-HOPO).

Preliminary tests in 2 M HCl solutions revealed that Sn^{4+} ions are complexed by 3,4,3-LI(1,2-HOPO) even though metal complexation is usually not favored at such high acidity due to competition with ligand protonation (Fig. S2, ESI†). The 1,2-HOPO chromophores absorb light in the UV, giving rise to a broad absorbance band centered at 301.5 nm, when protonated. This band is sensitive to metal binding, which usually induces a change in extinction coefficient as well as in the wavelength of maximum absorbance. Upon addition of 1 equivalent of SnCl$_4$ to a 3,4,3-LI(1,2-HOPO) solution in 2 M HCl, the broad absorbance band shifts from 301.5 nm to 299.5 nm and its extinction coefficient drops by about 30%. Concomitantly, the extinction coefficient in the region below 230 nm increases, as classically observed upon ligand–metal complexation.[11,32] Spectrophotometric titrations of the Sn(IV)–3,4,3-LI(1,2-HOPO) system between 0.1 M and 6.0 M HCl indicate that about 50% of Sn(IV) remain bound to 3,4,3-LI(1,2-HOPO) in 4 M HCl even when only 1 equivalent of chelator is used (Fig. S2, ESI†), and despite the presence of 100 000 equivalents of chloride ions. This feature suggests a remarkably stable complex, knowing that the four ligand pK_a's are comprised between 3.9 and 6.6[10] and that the chloride complexes of Sn(IV) are relatively stable (log β_{150} = 8.91).[21] Spectrophotometric titrations from pH 2 to 12 of samples containing a 1:1 mixture of Sn(IV) and 3,4,3-LI(1,2-HOPO) did not show any change in the absorption spectrum between pH 2 and 7.5 (Fig. S3, ESI†), confirming that Sn(IV) forms only one complex with 3,4,3-LI(1,2-HOPO) and that this species is stable

from very low pH (*i.e.* negative values) to near-neutral pH. Beyond pH 8, the UV-vis absorbance quickly transitions to that of the free ligand, concurrent with the formation of Sn(IV) hydroxide species. Formation of transient species [Sn^{IV}(OH)$_x$3,4,3-LI(1,2-HOPO)]$^{x-}$ may eventually happen within the pH range 8–10 but was not evaluated in the present study. High resolution mass spectrometry (HRMS) analysis of aqueous samples containing 1:1 mixtures of Sn(IV) and 3,4,3-LI(1,2-HOPO) confirmed the formation of a tetravalent complex (Fig. 1), as expected from the low standard redox potential of the Sn^{4+}/Sn^{2+} couple (E° = +0.38 V *vs.* SHE)[21] and the inherent selectivity of the ligand toward tetravalent ions; hypothetical Sn(II)–3,4,3-LI(1,2-HOPO) species are not expected to be thermodynamically stable in aqueous media without the presence of a strong reducing agent. The HRMS pattern observed for Sn(IV) is similar to what had been previously reported for Zr(IV), Th(IV), Pu(IV) and Bk(IV) complexes[13,14] of 3,4,3-LI(1,2-HOPO), with the ionization of the mono-charged proton, sodium, and potassium adducts containing 1 ligand and 1 metal ion. Based on the spectrophotometric measurements and HRMS data, formation of the neutral species [Sn^{IV}3,4,3-LI(1,2-HOPO)]^0 is presumed predominant from very low pH to near-neutral pH.

As previously reported, 3,4,3-LI(1,2-HOPO) complexes of tetravalent cations are so stable that classical methods, such as direct potentiometric titrations or ligand competitions using the common chelators DTPA or EDTA, cannot be applied to determine their stability constants. The stability of the Ce(IV) complex was nonetheless directly measured, by combining cyclic voltammetry and ligand competition batch titrations,[11] and using the highly stable [Ce^{IV}(NTA)$_2$]$^{2-}$ complex, whose stability had been reported in 2010,[33] as a reference. This allowed the subsequent determination of formation constants for the Th(IV), Zr(IV), and Pu(IV) complexes, with log β_{110} values ranging from 40.1 for Th(IV) to 43.5 for Pu(IV).[11,13] Building on this model, we used here the Zr(IV) complex as a reference for the assessment of the Sn(IV) species stability. Fig. 2 shows the spectrophotometric batch titration of a [Sn^{IV}3,4,3-LI(1,2-HOPO)]^0 solution, using a Zr(IV) challenge. Metal competition titrations were performed in highly acidic medium (0.4 M HCl) to match conditions previously used for the Zr(IV) system,[13] and to preclude metal hydrolysis. Upon addition of 1 equivalent of Zr(IV), the maximum absorbance wavelength gradually shifts from 299.5 to 302.0 nm and finally matches the reported Zr(IV) complex UV-vis spectrum. Three isosbestic points (261, 301, and 322 nm) were observed, confirming there is equilibrium between the two species. The reaction taking place during these metal-exchange titrations is defined in eqn (3), with a conditional constant log K of 3.18 $\pm$ 0.17 determined after refinement of the spectrophotometric data.

$$[\text{Sn}^{IV}3,4,3\text{-LI(1,2-HOPO)}]^0 + [\text{Zr(Cl)}_x]^{4-x}$$
$$= [\text{Zr}^{IV}3,4,3\text{-LI(1,2-HOPO)}]^0 + [\text{Sn(Cl)}_y]^{4-y} + (x - y)\text{Cl}^-$$

$$(3)$$
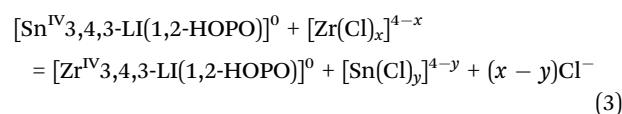
Despite the high respective stabilities of Sn(IV) chloride complexes (log β of 8.01 for SnCl$_4^-$ *versus* −1.51 for ZrCl$_4^-$)[21,22]
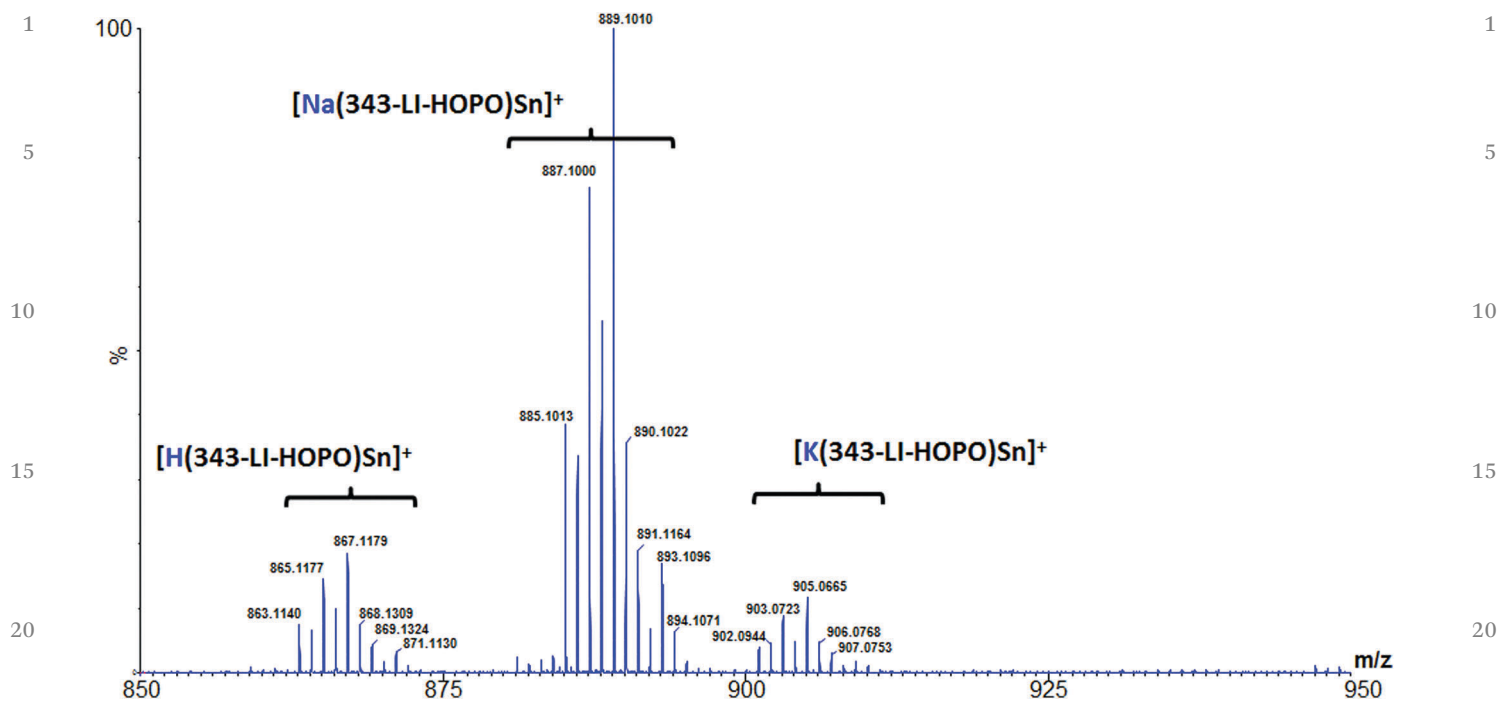
Fig. 1 High resolution mass spectrum of an aqueous solution containing 1 equivalent of $SnCl_4$ and 1 equivalent of 3,4,3-LI(1,2-HOPO). [Sn] = [3,4,3(LI-1,2-HOPO)] = 25 µM. The isotopic distribution matches that expected for Sn complexes. Media: 0.5% formic acid in water. Electrospray ionization, positive mode.
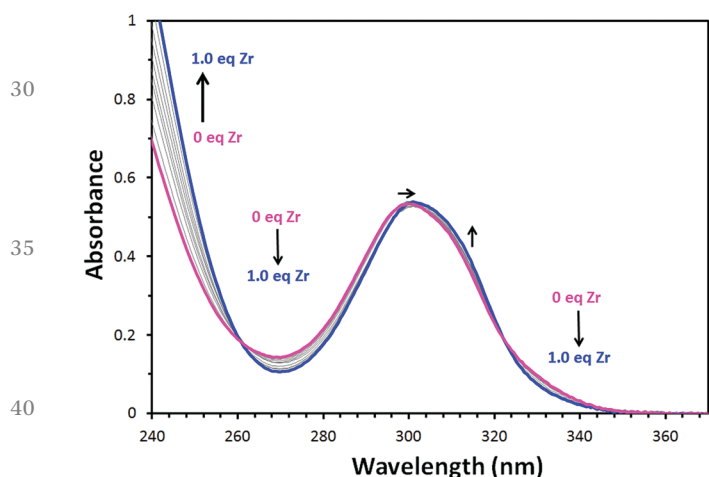

Fig. 2 Metal competition batch titration of $[Sn^{IV}3,4,3-LI(1,2-HOPO)]^0$ with Zr(ɪᴠ). [Sn] = [3,4,3(LI-1,2-HOPO)] = 30 µM, [Zr/Sn] = 0 to 1.0, I = 0.4 M (HCl), T = 20 °C. Path length: 10 mm. Arrows highlight changes in absorbance spectra due to the addition of Zr(ɪᴠ).

and $[Zr^{IV}3,4,3-LI(1,2-HOPO)]^0$ ($\log \beta_{110}$ = 43.1 ± 0.6),[13] the formation of $[Sn^{IV}3,4,3-LI(1,2-HOPO)]^0$ is favored, with a calculated constant $\log \beta_{110}$ = 46.6 ± 0.6. The Sn(ɪᴠ) complex is the most stable 3,4,3-LI(1,2-HOPO) species reported so far. Its extraordinary high stability constant is consistent with the complexation observed even under very acidic conditions, and in the same range as those exceptionally high values observed for other tetravalent metals. Based on literature data showing the high efficacy of 3,4,3-LI(1,2-HOPO) for the decorporation of

Pu(ɪᴠ) after internal contamination,[17] this ligand should be a very good *in vivo* chelator for Sn(ɪᴠ). The stability of the complex over a wide pH range could also be leveraged for Sn remediation in a broad variety of industrial effluents.

In spite of the large number of studies published on 3,4,3-LI(1,2-HOPO), only two crystal structures of this potent drug have been reported so far, for the $[Zr^{IV}3,4,3-LI(1,2-HOPO)]\cdot(MeOH)_{2.43}(H_2O)_{0.79}$ and $[KEu^{III}3,4,3-LI(1,2-HOPO)]\cdot DMF$ complexes.[16,34] The crystal structure of the unbound chelator is still unknown. Single crystals of $[Sn^{IV}3,4,3-LI(1,2-HOPO)\cdot3H_2O]$ were obtained from a wet methanol solution. The structure confirms the formation of octacoordinated and tetravalent tin species with the chelation of the metal ion through the four bidentate 1,2-HOPO units of the ligand (Fig. 3). Similar to the Eu(ɪɪɪ) and Zr(ɪᴠ) structures, the secondary amide groups and their three-carbon chain are positioned in *trans*
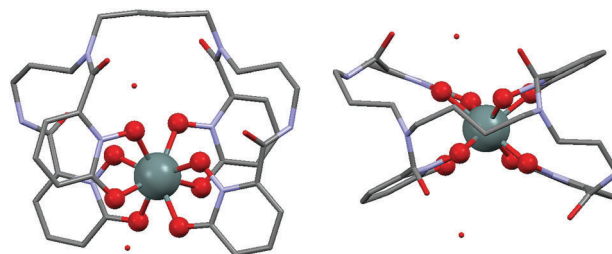

Fig. 3 Crystal structure of the 3,4,3-LI(1,2-HOPO) complex of Sn(ɪᴠ). Left: Side view. Right: Top view. The metal ion (grey) and the eight oxygen atoms (red) of the four 1,2-HOPO moieties are displayed as spheres. The rest of the chelator and the water molecules are depicted as capped sticks. Hydrogen atoms are omitted for clarity.

position relative to the central four-carbon chain of the spermine backbone, certainly limiting the steric hindrance. The Sn(IV) complex crystallizes in the chiral orthorhombic space group $C222_1$ as opposed to the centrosymmetric space groups $P2_1/c$ and $P\bar{1}$ for its Zr(IV) and Eu(III) analogues, respectively. The crystallographic parameters of the Sn(IV) complex are summarized in Table S1 (ESI†). Based on the measured absolute structure parameter of 0.001(6) for the single crystal selected for X-ray diffraction studies, it was evident that the two enantiomeric conformers of the Sn(IV) complex crystallize into separate domains under the growth conditions that were employed.

The Sn–O bond distances in the Sn(IV) complex range from 2.14 to 2.21 Å, slightly shorter than the reported Zr–O bonds of the same complex (2.17 to 2.24 Å), and in accordance with a ~0.03 Å difference between the ionic radii of the two metal ions. Interestingly, the two secondary amide functions, linking the spermine backbone and the terminal 1,2-HOPO moieties, are out of the plan of their 1,2-HOPO moiety for both the Sn(IV) and the Zr(IV) complexes whereas the secondary amides and their 1,2-HOPO groups are almost co-planar in the Eu(III) complex (Fig. S4, ESI†). The torsion angles between the terminal 1,2-HOPO plans and the corresponding secondary amide plans are 179.6° and 175.2° for the Eu(III) complex, with the C=O amide bonds pointing toward the outer part of the complex. In the case of Sn(IV), the two secondary C=O amide bonds are flipped by 111.6° relative to their 1,2-HOPO plan whereas the two torsion angles are 84.0° and 109.6° in the case of Zr(IV).

The Eu(III) complex of 3,4,3-LI(1,2-HOPO) has a formation constant log β_{110} of 20.2[30] and is about 25 orders of magnitude

less stable than its Sn(IV) and Zr(IV) counterparts. Hence, the stability of the metal complex seems to be reflected in the crystal structure by the torsion of the secondary amides. This feature seems counterintuitive since the rotation the amide group out of the aromatic 1,2-HOPO plan prevents π-conjugation between the two functionalities. The metal–ligand interactions in the Zr(IV) and Sn(IV) systems seem so strong that they overcome the stabilization of the ligand itself by π-conjugation. In all three crystal structures, the two internal 1,2-HOPO units are also out of the plane of their corresponding tertiary amide linker by 60°–80° and seem to systematically lose their π-conjugation upon binding to the metal ion. This indicates that the terminal 1,2-HOPO groups and their secondary amides are more sensitive to the nature of the metal ion and represent a good metric for metal-chelator interactions.

Lead(II) and cadmium(II) complexes

The solution thermodynamics of the Pb(II) and Cd(II) systems with 3,4,3-LI(1,2-HOPO) were also probed. To the best of our knowledge, hydroxypyridinone ligands have not yet been investigated for the chelation of these toxic heavy metals. In addition, the only metallic dication studied thus far with 3,4,3-LI(1,2-HOPO) is uranyl, UO_2^{2+}, mostly in the context of uranium decorporation.[12] UV-vis spectrophotometry and HRMS confirmed that both Cd(II) and Pb(II) ions are complexed by the ligand at physiological pH (Fig. 4 and Fig. S5, S6, ESI†). However, while Pb(II) can still interact with 3,4,3-LI(1,2-HOPO) at lower pH, Cd(II) remains totally unbound at pH 2, suggesting that the ligand has a lower affinity for Cd(II) than for Pb(II).
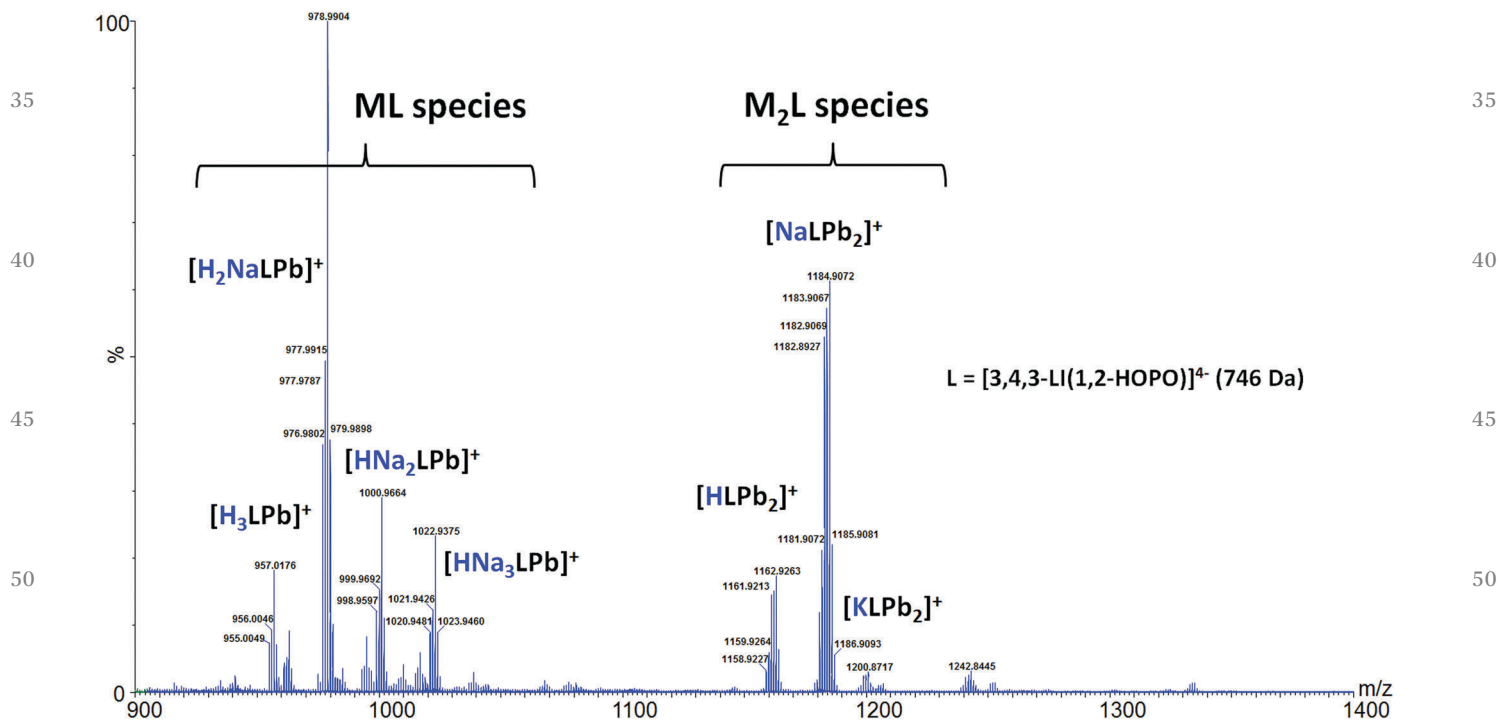

Fig. 4 High resolution mass spectra of aqueous solution containing 1 equivalent of PbCl₂ and 1 equivalent of 3,4,3-LI(1,2-HOPO). [(Pb)] = [3,4,3(LI-1,2-HOPO)] = 25 μM. Media: 0.5% formic acid in water. Electrospray ionization; positive mode. Similar results were obtained with CdCl₂ (Fig. S6, ESI†).
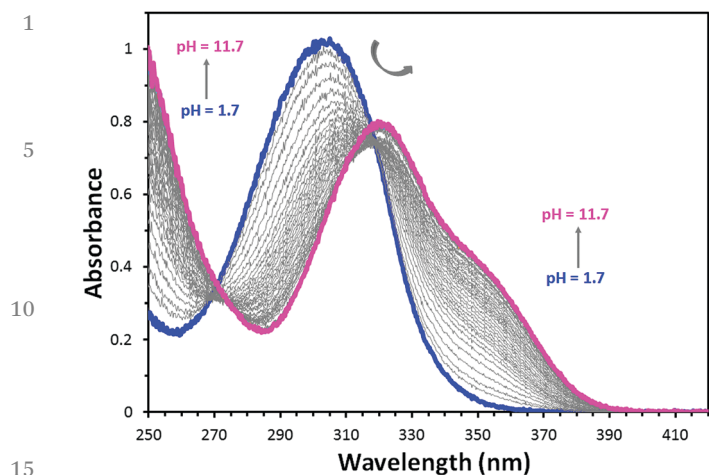
Fig. 5 Example of incremental spectrophotometric titration for the Pb(II)-3,4,3-LI(1,2-HOPO) system. 240 spectra measured between pH 1.7 and 11.7. I = 0.1 M (KCl). Buffer: 5 mM CH$_3$COOH, 5 mM CHES. T = 25 °C. Path length = 10 mm. Data abridged for clarity. Spectra corrected for dilution upon titrant addition. Similar results were obtained with CdCl$_2$ (Fig. S7, ESI†).

Table 1 Formation constants determined for the complexes of 3,4,3-LI(1,2-HOPO) (L) with Pb(II), Cd(II), and Sn(IV)

Species	$\log \beta_{MLH}$	Conditions
$[SnL]^0$	46.6 ± 0.6	0.4 M HCl, 20 °C
$[PbH_2L]$	24.82 ± 0.23	0.1 M KCl, 25 °C
$[PbHL]^-$	22.99 ± 0.21	
$[PbL]^{2-}$	18.04 ± 0.15	
$[Pb(OH)L]^{3-}$	7.41 ± 0.54	
$[Pb_2L]$	24.46 ± 0.22	
$[CdHL]^-$	20.21 ± 0.25	0.1 M KCl, 25 °C
$[CdL]^{2-}$	16.06 ± 0.25	
$[Cd(OH)L]^{3-}$	6.74 ± 0.08	
$[Cd_2L]$	20.38 ± 0.18	

This stands in stark contrast with tetravalent ions that remain bound to the chelator even at negative pH values. The HRMS patterns correspond to the ionization of the tri-adducts $[A_xB_{3-x}ML]^+$ (with A = H$^+$, B = Na$^+$ and M = Pb^{2+} or Cd^{2+}) in the positive mode and mono-adducts $[A'ML]^-$ (with A' = H$^+$, Na$^+$, or K$^+$) in the negative mode. The spectra also revealed the formation of bimetallic $[A'M_2L]^+$ species for both metals (Fig. 4), but more prominently in the case of Pb(II). This feature, not yet seen in other 3,4,3-LI(1,2-HOPO) systems, is thought to be due to the mismatch between the preferred hexacoordination mode of divalent Cd(II) and Pb(II) ions and the octadentate chelator. Such species may eventually be formed also for the uranyl system since UO$_2^{2+}$ does not require an octadentate ligand to complete its first coordination sphere but this has not yet been investigated.

Incremental spectrophotometric titrations of samples containing 1:1 mixtures of the divalent cations and the ligand between pH ∼ 1.7 and ∼12 (Fig. 5 and Fig. S7, ESI†) further revealed the formation of multiple complexes over this pH range. A speciation model adapted from that used for the UO$_2^{2+}$ system[12] was used to refine the spectrophotometric data. Accounting for the absorbance properties of the free ligand species, UV-vis absorbance changes were adequately fitted using four species in the case of Pb ($[PbH_2L]^0$, $[PbHL]^-$, $[PbL]^{2-}$, and $[Pb(OH)L]^{3-}$) and three species in the case of Cd ($[CdHL]^-$, $[CdL]^{2-}$, and $[Cd(OH)L]^{3-}$). The formation constants of these 1:1 species are summarized in Table 1 and speciation diagrams are provided in Fig. S8 (ESI†). The stability of the $[PbL]^{2-}$ species is in the same range as that reported for the corresponding UO$_2^{2+}$ complex,[12] suggesting 3,4,3-LI(1,2-HOPO) may be a candidate chelator for lead decorporation but also that hexadentate structures such as the TREN-based hydroxypyridinone ligands developed for MRI contrast agents,[35] could display even higher affinity for Pb(II). The Cd(II) species are less stable than their Pb(II) counterparts by about two orders of magnitude (Table 1), likely due to the softer character of Cd(II).[1]
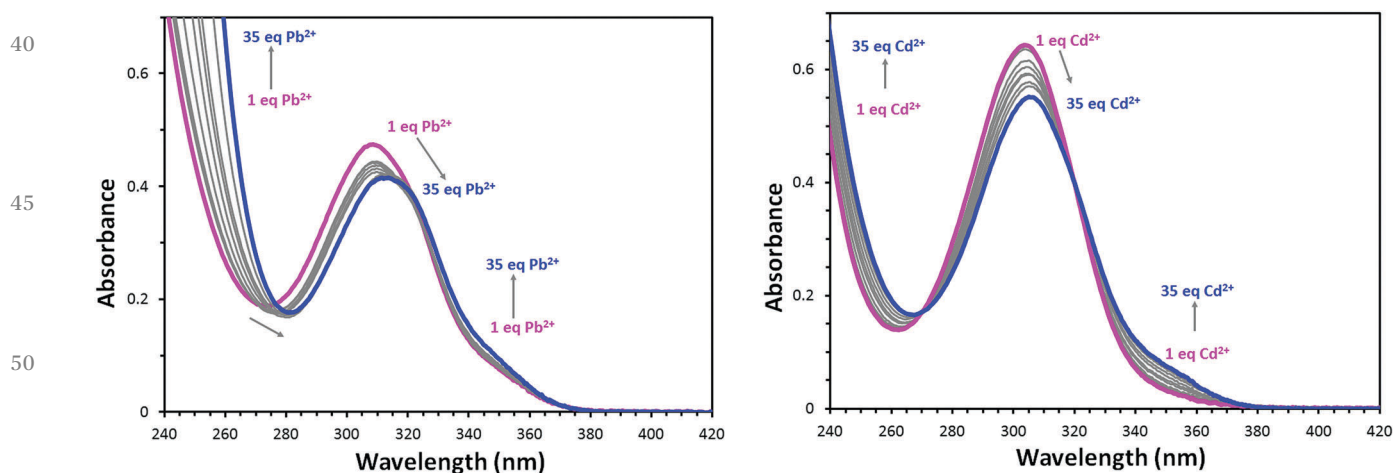

Fig. 6 Left: Changes in the UV-vis spectrum of $[PbLH]^-$ complex (L = 3,4,3-LI(1,2-HOPO)$^{4-}$) upon addition of PbCl$_2$. Right: Changes in the UV-vis spectrum of $[CdLH]^-$ complex upon addition of CdCl$_2$. [L] total = 29 μM, [M] = 1 to 35 equivalents. Buffer: 10 mM formic acid, pH 3.3 to 3.4. I = 0.1 M (KCl), T = 25 °C. Path length = 10 mm.

This lower binding affinity of the ligand for Cd(II) is reflected by the absence of $[CdH_2L]^0$ formation in the lower pH range, in accordance with early results showing that Cd(II) ions are not bound to 3,4,3-LI(1,2-HOPO) at pH 2. While 3,4,3-LI(1,2-HOPO) may still potentially be useful for Cd decorporation applications at physiological pH, softer hexadentate analog structures should be explored.

The stability constants of the bimetallic 2 : 1 complexes were evaluated through spectrophotometric titrations performed at fixed pH (Fig. 6). The incremental addition of metal ions to a 1 : 1 metal : chelator mixture induces UV-vis absorbance changes, with resulting spectra that do not match any of those observed for the 1 : 1 mixtures over the pH range 1.5–12 but can be modeled according to eqn (4). The Pb(II) system was found more sensitive to the ratio metal : chelator, suggesting that 3,4,3-LI(1,2-HOPO) is more prone to form bimetallic species with Pb(II) than with Cd(II), in line with the results obtained by HRMS.

$$[MLH]^- + M_{(aq)}^{2+} = [M_2L] + H^+ \qquad (4)$$
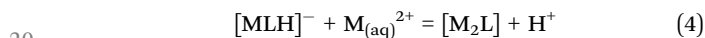
Refinement of the titration data yielded $\log \beta_{210}$ values of 24.5 for Pb(II) and 20.4 for Cd(II). The octadentate ligand is therefore more prone to form bimetallic species with Pb than with Cd, which reflects the generally higher affinity of the ligand for Pb(II). The calculated percentage of bimetallic species as a function of the ligand : metal ratio is given in Fig. S9 (ESI†) and shows that a 10-fold excess of Pb(II) is enough to totally saturate 3,4,3-LI-(1,2-HOPO), whereas a 100-fold excess is required in the case of Cd(II).

Lead(II) *in vivo* decorporation

Based on the *in vitro* solution thermodynamic results discussed above, the efficacy of 3,4,3-LI(1,2-HOPO) at promoting Pb(II) decorporation in mice was evaluated. The designed experimental protocols used ^{210}Pb (100% beta emitter, $t_{1/2}$ = 22.2 years) as a radiotracer, as well as CaNa$_2$EDTA-treated and untreated control groups. The radiolabel ^{210}Pb was administered intravenously (iv) as a citrate solution and the ligands were injected intraperitoneally (ip) from 24 h before to 48 h after metal contamination. Mice were euthanized 4 d after the metal injection, and tissues and excreta were radioanalyzed for ^{210}Pb content (see Fig. 7 and Fig. S10, S11, ESI†). Significant ^{210}Pb elimination enhancement was observed in the CaNa$_2$EDTA-treated group as well as in groups treated with prophylactic 3,4,3-LI(1,2-HOPO) at 1 or 6 h before metal contamination, in comparison to the saline-injected control group (Fig. 7, Panel A). These respective decreases in total body burden were correlated to significant decreases in skeleton ^{210}Pb burdens (Fig. S10, Panel D, ESI†). However, there were no other notable significant changes in ^{210}Pb content at the single organ level, to the exception of a large and significantly increased ^{210}Pb amount in the liver of the group showing the best decorporation efficacy, which was prophylactically treated with 3,4,3-LI(1,2-HOPO) 1 h before metal contamination (Fig. S10, Panel B, ESI†). This large liver content is likely reflecting a
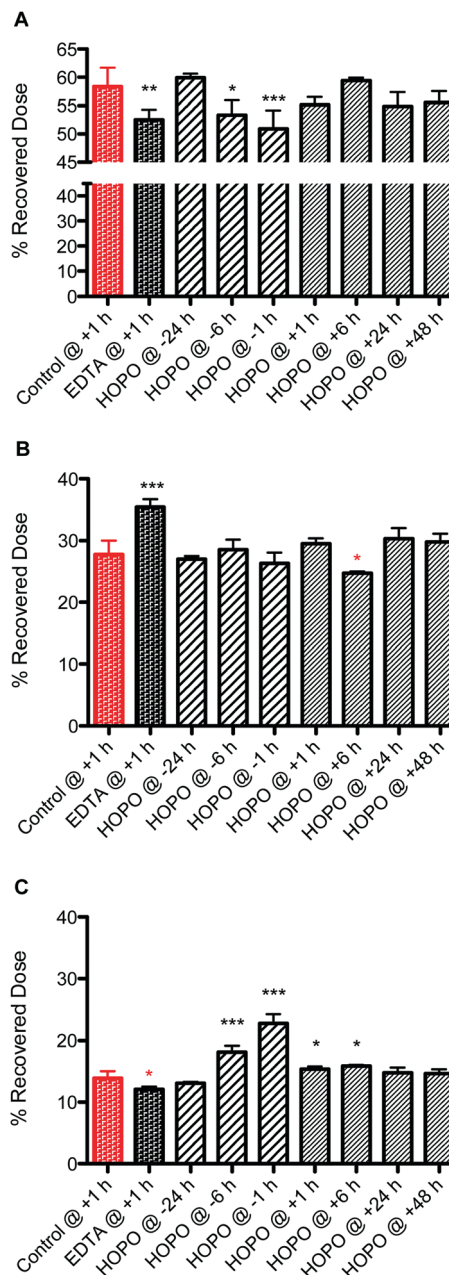

Fig. 7 Total ^{210}Pb body content (A), urine (B), and fecal (C) outputs at 4 days after metal challenge, preceded or followed by a single ip chelation treatment. Young adult female Swiss-Webster mice were injected iv with ^{210}Pb-citrate; saline (red) or treatment (black, 3,4,3-LI(1,2-HOPO) or Ca–ETDA [100 µmol kg^{-1}] was administered ip at 1 h, 6 h, or 24 h before or at 1 h, 6 h, 24 h, or 48 h after contamination); mice were euthanized 4 days after metal challenge. Data expressed as percent of recovered ^{210}Pb dose (% RD, mean ± SD) for each four-mouse group. Groups with significantly different retention and excreta output than for control mice are indicated by *, **, or *** ($p < 0.05$, $p < 0.01$, or $p < 0.001$, 1-way ANOVA with *post hoc* Dunnett's multiple comparison test).

fraction of ^{210}Pb that is on the path to excretion: as expected from the large body of f-element decorporation data available with 3,4,3-LI(1,2-HOPO), this ligand promoted ^{210}Pb decorporation solely through fecal excretion (∼46% of total excretion and 100% of enhanced excretion from biliary fraction), in contrast

to the predominant urinary profiles seen in control and CaNa$_2$EDTA-treated ($\sim$25% of total excretion and 0% of enhanced excretion from biliary fraction) groups (Fig. 7, Panels B and C). Daily and cumulative excretion profiles further highlight these differences (Fig. S11, ESI†): while CaNa$_2$EDTA is effective at enhancing ^{210}Pb elimination promptly, the spike observed in the urines for that group at 1 day post metal contamination is not sustained and the elimination kinetics quickly resemble those of the control group. In contrast, the biliary excretion path promoted by 3,4,3-LI(1,2-HOPO) is sustained over several days, with the patterns of cumulative excretion relative to control not yet reaching a plateau after 4 days, which suggests that one treatment of 3,4,3-LI(1,2-HOPO) may be more efficacious over time. Overall, these results corroborate the similar thermodynamic stability constants corresponding to the Pb(II) complexes of EDTA and 3,4,3-LI(1,2-HOPO), with comparable efficacy at promoting *in vivo* ^{210}Pb removal. It is however important to note the differences in excretion profiles for both ligands, which combined with the recognized lack of toxicity of 3,4,3-LI(1,2-HOPO) would warrant exploring further the use of hydroxypyridinone ligands to treat Pb contamination and optimizing the 3,4,3-LI(1,2-HOPO) architecture to more specifically target metals that exhibit lower coordination numbers and softer characters than f-elements.

Conclusion

The interactions between the octadentate hydroxypyridinonate ligand 3,4,3-LI(1,2-HOPO) and heavy metal ions Sn^{4+}, Pb^{2+}, and Cd^{2+} were investigated in aqueous solutions. The ligand exhibits a remarkable affinity toward Sn^{4+}, with the formation of an octacoordinated Sn(IV) species that is stable from very acidic (pH < 0) to slightly basic conditions. The high stability constant of the [Sn^{IV}3,4,3-LI(1,2-HOPO)]^0 complex is in the same range as those observed for much larger tetravalent actinide ions such as Pu(IV). The corresponding solid state structure revealed a chiral crystalline phase, and the structural parameters of the Sn(IV) complex were compared to those of its Eu(III) and Zr(IV) analogues in the context of their relative stabilities in solution. In addition, 3,4,3-LI(1,2-HOPO) displays a relatively high affinity for Pb^{2+} and Cd^{2+} ions even though this ligand was not designed nor optimized for these hexacoordinated and soft cations. The observed binding capacity of the 1,2-HOPO ligand for Pb and Cd provides the basis for a new class of chelators that would be based on hydroxypyridinonate binding units. Future work[36] will focus on designing derivatives inspired from 3,4,3-LI(1,2-HOPO) and tuned to match the hexacoordinated mode and softness of Pb and Cd ions.

Conflicts of interest

Q6

Acknowledgements

References

1 O. Andersen, *Environ. Health Perspect.*, 1984, **54**, 249–266.
2 M. M. Jones and M. G. Cherian, *Toxicology*, 1990, **62**, 1–25.
3 P. Goovaerts, *Sci. Total Environ*, 2017, **581–582**, 66–79.
4 T. M. Olson, M. Wax, J. Yonts, K. Heidecorn, S.-J. Haig, D. Yeoman, Z. Hayes, L. Raskin and B. R. Ellis, *Environ. Sci. Technol. Lett.*, 2017, **4**, 356–361.
5 S. Zahran, S. P. McElmurry and R. C. Sadler, *Environ. Res.*, 2017, **157**, 160–172.
6 Environmental Defense Fund, *Lead in food: A hidden health threat*, Environmental Defense Fund, 2017.
7 R. A. Bernhoft, *Sci. World J.*, 2013, **2013**, 1–7.
8 G. F. Nordberg, B. F. Fowler, M. Nordberg and L. Friberg, *Handbook on the Toxicology of Metals*, Elsevier, Amsterdam, Netherlands, 3rd edn, 2007, pp. 445–486.
9 S. Blunden and T. Wallace, *Food Chem. Toxicol.*, 2003, **41**, 1651–1662.
10 R. J. Abergel, A. D'Aléo, C. Ng Pak Leung, D. K. Shuh and K. N. Raymond, *Inorg. Chem.*, 2009, **48**, 10868–10870.
11 G. J.-P. Deblonde, M. Sturzbecher-Hoehne and R. J. Abergel, *Inorg. Chem.*, 2013, **52**, 8805–8811.
12 M. Sturzbecher-Hoehne, G. J.-P. Deblonde and R. J. Abergel, *Radiochim. Acta*, 2013, **101**, 359–366.
13 M. Sturzbecher-Hoehne, T. A. Choi and R. J. Abergel, *Inorg. Chem.*, 2015, **54**, 3462–3468.
14 G. J.-P. Deblonde, M. Sturzbecher-Hoehne, P. B. Rupert, D. D. An, M.-C. Illy, C. Y. Ralston, J. Brabec, W. A. de Jong, R. K. Strong and R. J. Abergel, *Nat. Chem.*, DOI: 10.1038/nchem.2759. Q7
15 M. A. Deri, S. Ponnala, B. M. Zeglis, G. Pohl, J. J. Dannenberg, J. S. Lewis and L. C. Francesconi, *J. Med. Chem.*, 2014, **57**, 4849–4860.
16 M. A. Deri, S. Ponnala, P. Kozlowski, B. P. Burton-Pye, H. T. Cicek, J. S. Lewis and L. C. Francesconi, *Bioconjugate Chem.*, 2015, **26**, 2579–2591.
17 R. J. Abergel, P. W. Durbin, B. Kullgren, S. N. Ebbe, J. Xu, P. Y. Chang, D. I. Bunin, E. A. Blakely, K. A. Bjornstad, C. J. Rosen, D. K. Shuh and K. N. Raymond, *Health Phys.*, 2010, **99**, 401–407.
18 P. Gans and B. O'Sullivan, *Talanta*, 2000, **51**, 33–37.
19 P. Gans, A. Sabatini and A. Vacca, *Talanta*, 1996, 1739–1753.

20 A. E. Martell, R. M. Smith and R. J. Motekaitis, *NIST standard reference database 46*. National Institute of Standards and Technology, Gaithersburg, MD.

21 Organisation for Economic Co-operation and Development, *Chemical Thermodynamics of Tin*, OECD Publishing, Paris, 2012, vol. 12.

22 F. J. Mompean, J. Perrone and M. Illemassène, *Chemical thermodynamics of zirconium*, Gulf Professional Publishing, 2005, vol. 8.

23 Bruker, *SADABS, APEX3, and SAINT*, Bruker AXS, Madison, Wisconsin, USA.

24 G. M. Sheldrick, *Acta Crystallogr., Sect. A: Found. Crystallogr.*, 2008, **64**, 112–122.

25 L. J. Farrugia, *J. Appl. Crystallogr.*, 2012, **45**, 849–854.

26 C. F. Macrae, I. J. Bruno, J. A. Chisholm, P. R. Edgington, P. McCabe, E. Pidcock, L. Rodriguez-Monge, R. Taylor, J. van de Streek and P. A. Wood, *J. Appl. Crystallogr.*, 2008, **41**, 466–470.

27 P. W. Durbin, B. Kullgren, S. N. Ebbe, J. Xu and K. N. Raymond, *Health Phys.*, 2000, **78**, 511–521.

28 P. W. Durbin, N. Jeung, B. Kullgren and G. K. Clemons, *Health Phys.*, 1992, **63**, 427–442.

29 D. D. An, B. Kullgren, E. E. Jarvis and R. J. Abergel, *Chem. – Biol. Interact.*, 2017, **267**, 80–88.

30 M. Sturzbecher-Hoehne, C. Ng Pak Leung, A. D'Aléo, B. Kullgren, A.-L. Prigent, D. K. Shuh, K. N. Raymond and R. J. Abergel, *Dalton Trans.*, 2011, **40**, 8340.

31 R. Shannon, *Acta Crystallogr., Sect. A: Found. Crystallogr.*, 1976, **32**, 751–767.

32 J. Xu, B. O'Sulliva and K. N. Raymond, *Inorg. Chem.*, 2002, **41**, 6731–6742.

33 Y. Suzuki, T. Nankawa, A. J. Francis and T. Ohnuki, *Radiochim. Acta*, DOI: 10.1524/ract.2010.1735.

34 L. J. Daumann, D. S. Tatum, B. E. R. Snyder, C. Ni, G. Law, E. I. Solomon and K. N. Raymond, *J. Am. Chem. Soc.*, 2015, **137**, 2816–2819.

35 C. J. Jocher, M. Botta, S. Avedano, E. G. Moore, J. Xu, S. Aime and K. N. Raymond, *Inorg. Chem.*, 2007, **46**, 4796–4798.

36 R. J. Abergel and G. J.-P. Deblonde, Patent Pending, 2016. Q8